Effects of selenisation temperature on photoluminescence and photoluminescence excitation spectra of ZnO/CdS/Cu$_2$ZnSnSe$_4$/Mo/glass

M.A. Sulimov[1,2], M.V. Yakushev[1,2,3], J. Márquez-Prieto[4], I. Forbes[4], P.R. Edwards[5], V.D. Zhivulko[6], O.M. Borodavchenko[6], A.V. Mudryi[6], J. Krustok[7] and R.W. Martin[5]

[1]M.N. Mikheev Institute of Metal Physics UB RAS, 620108, S. Kovalevskaya Street 18, Ekaterinburg, Russia

[2]Ural Federal University, Mira 19, 620002 Ekaterinburg, Russia

[3]Institute of Solid State Chemistry of Ural Branch of the RAS, Pervomaiskaya 91, 620990 Ekaterinburg, Russia

[4]Northumbria Photovoltaic Application Group, Faculty of Engineering and Environment, Northumbria University, Ellison Place, Newcastle upon Tyne NE1 8ST, UK

[5]Department of Physics, SUPA, University of Strathclyde, Rottenrow 107, G4 0NG Glasgow, UK

[6]Scientific-Practical Material Research Centre of the National Academy of Science of Belarus, P.Brovki 19, 220072 Minsk, Belarus

[7]Tallinn University of Technology, Departments of Physics and Materials Science, Ehitajate tee 5, 19086 Tallinn, Estonia

E-mail: michael.yakushev@strath.ac.uk

ABSTRACT

The effect of solar cell processing (including etching in KCN along with deposition of CdS and ZnO) on photoluminescence (PL) spectra and bandgap E_g (measured at 4.2 K by photoluminescence excitation) of $Cu_2ZnSnSe_4$ films, produced by selenising metallic precursors at 450°C, 500°C and 550°C, was studied. Temperature and excitation intensity analysis of the P1 dominant band in the PL spectra of solar cells suggests that after processing this band still can be assigned to the free-to-bound recombination of free electrons with holes bound at deep acceptor levels influenced by valence band-tails. However processing increased the intensity of P1 and blue shifted it. The strongest effect was observed for the film selenised at 500°C. For the film selenised at 450°C the blue shift and increase in the intensity were smaller and only a slight intensity rise was found for the film selenised at 550°C. The intensity increase we assign to a reduction in the concentration of non-radiative recombination centers on the surface because of the etching and changes in doping due to inter-diffusion of Cd, S, Se and Zn after the deposition of CdS. Such an inter-diffusion depends on the elemental composition of the films defining the chemistry of defects and influencing E_g which increased in the film selenised at 500°C but decreased in the other films. Processing increased the P1 shift rate (*j*-shift) with excitation power change in all the films demonstrating a higher compensation degree in the solar cells which is consistent with the formation of an interface layer containing new donors Cd_{Cu}.

Keywords: Copper zinc tin selenide; Solar cells; Photoluminescence; Selenisation; Optical spectroscopy

1. Introduction

The quaternary semiconductor $Cu_2ZnSnSe_4$ (CZTSe) with the kesterite structure is used as the absorber layer of sustainable thin film solar cells [1]. This material has a direct bandgap suitable for solar energy conversion and an absorption coefficient greater than $10^4 cm^{-1}$.

CZTSe is successfully employed in solar cells with a record conversion efficiency of 11.6% [2] for laboratory size devices. Further improvements depend on increasing the knowledge of the electronic properties, namely, the nature of defects and their relation with growth conditions. One of the most important conditions is the selenisation temperature (ST). The effect of selenisation temperature on the photoluminescence (PL) spectra of CZTSe thin films has recently been reported [3]. The authors also tried to correlate these properties with the performance of solar cells, fabricated from these films. However to understand better the effect of selenisation temperature one should take in account the influence of solar cell processing, etching of the as deposited films with KCN as well as the deposition of CdS and ZnO.

PL is a useful characterisation technique to analyse the electronic properties of semiconductors [4]. Mechanisms of radiative recombination critically depend on the doping and compensation levels. In the kesterites high concentrations of charged defects generate spatial potential fluctuations resulting in band-tails [5,6]. The hole effective mass of CZTSe is significantly greater than that of electrons [7] so at high concentrations of *n*- and *p*-type defects this material becomes highly doped in terms of donors whereas in terms of acceptors it behaves as a conventional semiconductor. To

achieve the condition of high doping in the kesterites the acceptor concentration should be 17 times higher than that of donors [8]. According to the model, developed in ref. [9] and applied to interpret PL spectra of Cu(InGa)Se$_2$ [10] and CZTSe [3,5,11] at low temperatures we can expect: (1) band-to-tail transitions involving the recombination of holes, localised at acceptor-like states of the valence band tail, with free electrons and (2) free-to-bound (FB) transitions involving the recombination of free electrons with holes localised at acceptors, which are deeper than the mean energy depth of potential fluctuations γ. A band-to-band (BB) transition, the recombination of free holes and free electrons is likely to become visible at higher temperatures. In this paper we study the effect of ST on PL and photoluminescence excitation (PLE) spectra of CZTSe-based solar cells and compare them with those of as deposited CZTSe films on Mo/Glass substrates.

2. Experimental details

Thin films of CZTSe were fabricated at Northumbria University. A set of 450 nm thick multilayer Cu–Zn–Sn metallic precursors, made of several nanometres thick alternating Cu, Zn and Sn layers, were sequentially deposited on the Mo/glass substrates (held on a rotating table) at room temperature by a three-target magnetron Nordiko 2000 sputtering high-purity (5N) Cu, Zn and Sn targets of 150 mm diameter at the Argon pressure of 3×10^{-3} Torr (0.4 Pa). A power of 70 W, 120 W and 140 W was applied to the Zn, Cu and Sn targets, respectively. These precursors were then selenised in graphite boxes containing Se pellets in a Rapid Thermal Processor (Annealsys AS-One)

by a two-step thermal annealing for 5 and 15 min, respectively, at a base pressure of 85 kPa of nitrogen. The graphite boxes were then heated in a Rapid Thermal Processor (Annealsys AS-One) at 300 °C (the first step) and then the second at 450 °C, 500 °C or 550 °C for films 1 (solar cell 1), 2 (solar cell 2) and 3 (solar cell 3), respectively. More information on the process of the film fabrication can be found elsewhere [3,11,12]. The CdS buffer layer was grown using a standard chemical bath deposition (CBD) process at 70°C after etching the films with a 10 wt% KCN solution for 30 seconds. Solar cells with an area of $3x3mm^2$ were then fabricated by DC-magnetron deposition of ZnO/ZnO:Al transparent front contacts and mechanical scribing. The principal device parameters measured under simulated AM1.5 solar illumination (100 mW/cm^2, 25°C) for cells fabricated from films 1 and 2 are shown in Table 1. Electrical measurements could not be performed on solar cells with the film 3 absorber, where the Mo back contact was completely selenised.

The elemental compositions of the films, determined by wavelength dispersive X-ray microanalysis as the average of 10-point linear scans across the films, are shown in Table 1. These values have been reported earlier in ref. [3]. The structural properties and the presence of secondary phases, studied using room temperature Raman scattering and X-ray diffraction, as well as scanning electron microscope micrographs of the films used for the solar cells fabrication have also been reported earlier [3].

Table 1 The [Cu]/[Zn+Sn] and [Zn]/[Sn] ratios of the films and parameters of the solar cells fabricated from them (data reproduced from [3]).

Selenisation	450°C	500°C	550°C

temperature			
[Cu]/[Zn + Sn]	0.76 ± 0.08	0.78 ± 0.10	0.83 ± 0.04
[Zn]/[Sn]	0.92 ± 0.17	1.18 ± 0.02	1.17 ± 0.06
V_{OC} (mV)	336	421	
J_{SC} (mA/cm^2)	26.5	30.2	
FF	35.2	58.0	
η (%)	3.2	7.4	

The PL measurements were carried out using a 1 m focal length single grating monochromator and the 514 nm line of a 300 mW Ar$^+$ laser. A closed-cycle helium cryostat was employed to measure the PL spectra at temperatures from 6 K to 300 K. The dispersed PL signal was detected by an InGaAs photomultiplier tube (PMT), sensitive from 0.9 µm to 1.65 µm. More experimental details can be found in Ref. [3,11].

The PLE measurements were carried out using a 0.6 m focal length single grating monochromator with, an InGaAs photodiode sensitive from 0.9 µm to 1.9 µm and a liquid helium bath cryostat. A combination of a 400 W halogen tungsten lamp with 0.3 m focal length single grating monochromator was used for excitation. The PLE spectra were recorded by detecting the signal at the energy near the maximum intensity of the

dominant PL bands: 0.95 eV for solar cell 1, 0.96 eV for solar cell 2 and 0.90 eV for solar cell 3. More experimental details can be found in Ref. [3,11] .

3. Results and discussion

PL spectra of the three solar cells, measured at 6 K under experimental conditions equivalent to those used for such measurements of the as deposited films in ref. [3], are shown in Fig. 1. These spectra are dominated by an asymmetric band P1 with peak energy at 0.95 eV, 0.96 eV and 0.90 eV, respectively. The PL intensity of the dominant band, measured at 6 K, at first increases by a factor of two as the selenisation temperature rises from 450°C to 500°C but then falls down by a factor of four for a selenisation temperature of 550°C. Apart from the dominant band the PL spectra contain a broad high energy band P3 at 1.3 eV. The spectra show only the low energy part of this band whose high energy side is beyond the sensitivity limit of the detector used.
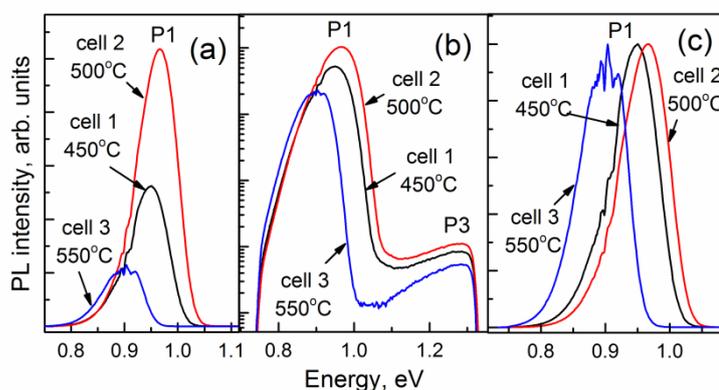
Fig. 1. PL spectra of solar cells (1), (2) and (3) measured at 6 K using similar optical alignments and laser excitation on a linear (a,c) and logarithmic (b) intensity scale. Normalised P1 band (c).

The excitation intensity dependence of the PL spectra for the three samples is shown in Fig. 2. The integrated intensity $I(P)$ under the dominant band depends on the excitation laser power P as $I \sim P^k$. Thereby we determine k power coefficients by measuring the slope of log-log plots of $I(P)$. Values of k 1.01 ± 0.01, 0.95 ± 0.02 and 0.97 ± 0.01 were estimated for solar cells 1, 2 and 3, respectively, as shown in Table 2. Radiative recombination of charge carriers localised at defects whose energy levels lie within the bandgap is indicated by k values smaller than unity whereas k values greater than unity suggest that the recombination does not involve localisation at defects [13]. In the kesterites k values greater than unity can be expected for the BB mechanism [3,11,14]. The determined values of k suggest that at low temperatures the dominant PL bands might include unresolved BB peaks.
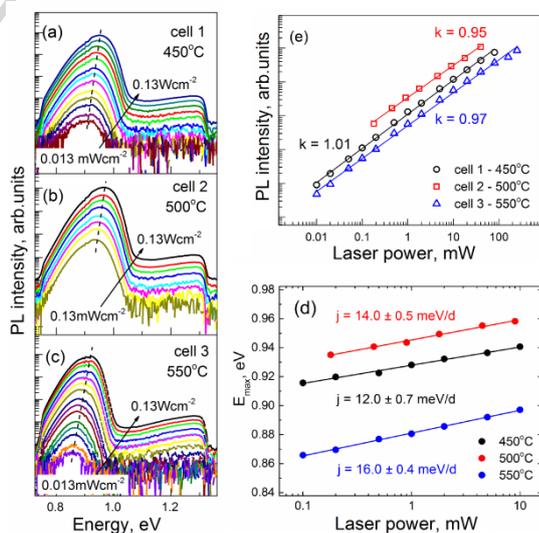
Fig. 2. Excitation intensity dependencies of the PL spectra of the solar cells with selenisation temperatures of 450°C (a), 500°C (b) and 550°C (c) measured at 6 K. The dependence of peak position on excitation laser power P (d). The dependence of the integrated PL intensity on excitation laser power P (e).

The dominant bands in all the three samples show significant blue shifts with increasing laser power, whereas their shapes do not change. The j-shifts (the rate of the shift per decade of increase of the laser power) increases from 12.0±0.7 meV to 14.0±0.5 meV per decade for solar cells 1 and 2 and then to 16.0±0.4 meV per decade for solar cells 3. Such significant j-shifts of the dominant band, along with its asymmetric shape at low temperatures, are characteristics of band-tail related recombination mechanisms [9,10].

Table 2 Spectral energy and FWHM of the dominant PL band at 6 K, bandgaps E_g, average depths of potential fluctuations γ and activation energies E_a of the temperature quenching of the dominant bands for solar cells 1, 2 and 3.

Selen.Temp.	450°C		500°C		550°C	
sample	film 1	cell 1	film 2	cell 2	film 3	cell 3
E_{max}, eV	0.93	0.95	0.94	0.96	0.90	0.90
FWHM, meV	84	85	84	87	100	83
j-shift,	11	12	12	14	15	16

meV/dec.						
k	1.0	1.0	1.0	1.0	1.0	1.0
E_g, eV	1.05	1.06	1.03	1.02	1.05	1.02
γ, meV	24	24	24	24	27	21
E_a, meV	55	65	55	70	70	75

The temperature dependencies for the solar cells were measured at the same optical conditions. The evolution of the normalised PL spectra of the three solar cells with rising temperature is shown in Fig. 3 on a linear scale. The P1 PL band reveals clear red shifts with increasing temperature in all the three samples. Such shifts can be taken as a confirmation of the band-tail related nature of this emission [9,10]. Increasing temperature thermalises the holes at shallower states of the acceptor-like states of the valence band-tail into the valence band whereas holes at deeper states remain localised. This process red shifts the P1 band maximum whereas the recombination of holes, thermalised to the valence band with free electrons, forms the BB band.
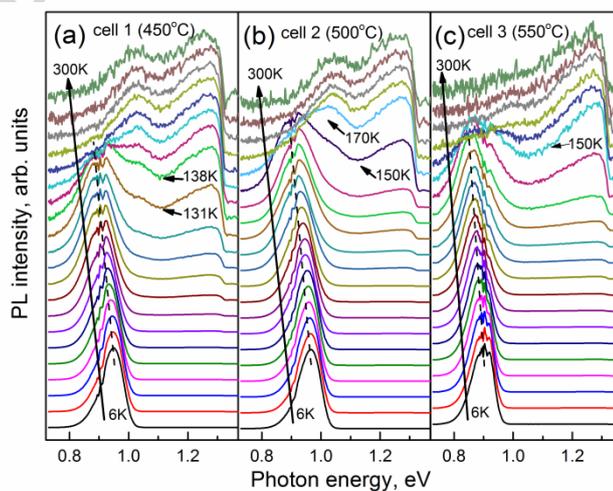
Fig. 3. Evolution of the normalised temperature dependence of the PL spectra of cell 1, 2 and 3. The spectra are shifted along the y-axis for clarity.

The temperature dependence of the PL spectra is shown in Fig. 4 on a logarithmic scale. It can be seen that the dominant P1 band gradually quenches by 170 K, 200 K and 180 K for the solar cell 1, 2 and 3, respectively, making possible to see the P2 band at high temperature. Its spectral position is very close to E_g. Therefore it may be a BB recombination. At low temperatures the shape of the P1 band is asymmetric whereas with increasing temperature this band becomes more symmetric. The temperature dependence of the spectral energy of the PL intensity maxima $E_{max}(T)$ for the P1 bands is presented in Fig. 4. It can be seen that with rising temperature all the bands shift to lower energies. PLE spectra were used to determine the bandgap of the films at 4.2 K. The absorbance $\alpha(h\nu)$, where $h\nu$ is photon energy, is determined from the low energy side of the PLE spectra. This side has been fitted with sigmoidal functions proposed in [15] $a(h\nu) = a0/[1+\exp(E_g - h\nu)/\Delta E]$, where $h\nu$ is the photon energy, $\alpha0$ vertical scale parameter and ΔE a broadening energy [16]. The determined values of the bandgap of CZTSe in the cells are 1.06±0.01 eV, 1.02±0.01 eV and 1.02±0.01 eV for the cells (1), (2) and (3), respectively, as presented in Table 2.
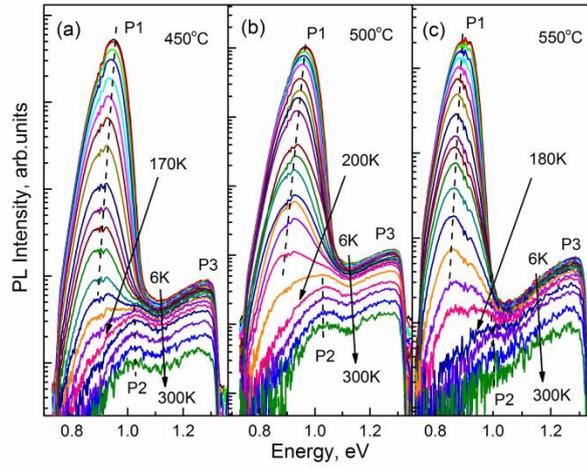
Fig. 4. Temperature dependencies of the PL spectra of the solar cells with the selenisation temperature of 450°C (a), 500°C (b) and 550°C (c).

All the experimental PL spectra were fitted with an empirical asymmetric double sigmoid function (DSF) proposed in [10] for band-tail related recombination:

$$I(hv) = A\left(1 \Big/ \left(1 + \exp\left[-\left(\frac{hv - E_1}{W_1}\right)\right]\right)\right)\left(1 - 1\Big/\left(1 + \exp\left[-\left(\frac{hv - E_2}{W_2}\right)\right]\right)\right). \tag{1}$$

where A, E_1, E_2, W_1 and W_2 are the experimental parameters. E_1 and W_1 represent the shape of the low-energy side of the PL bands while E_2 and W_2 belong to the high-energy side. Example of the fitting of the PL, measured at 6 K, for the three cells are shown in Fig. 5(a,b,c) whereas the temperature dependence of W_1 and W_2 is shown in Fig.5(d). The $W1$ parameter specifies the average depth of potential fluctuations (γ). It shows little change with temperature rise up to 50 K.

The average depth of potential fluctuations (γ), determined from the low energy side of the dominant bands, was estimated to be of 24±2 meV for selenisation temperatures 450°C and 500°C whereas for 550°C γ falls down to 21±2 meV. The use of fitted DSFs

improves the accuracy of the dominant band temperature dependence analysis providing an opportunity to subtract one PL band from the other and allow evaluation of the evolution of poorly resolved and unresolved PL bands with increasing temperature. Examples of the fitting of DSF at different temperatures are shown in Fig. 6. The P1 band quenches by temperatures of 200 K whereas the BB band can be observed resolved at temperatures above 150 K. The P3 peak becomes dominant at temperatures in excess of 150 K.
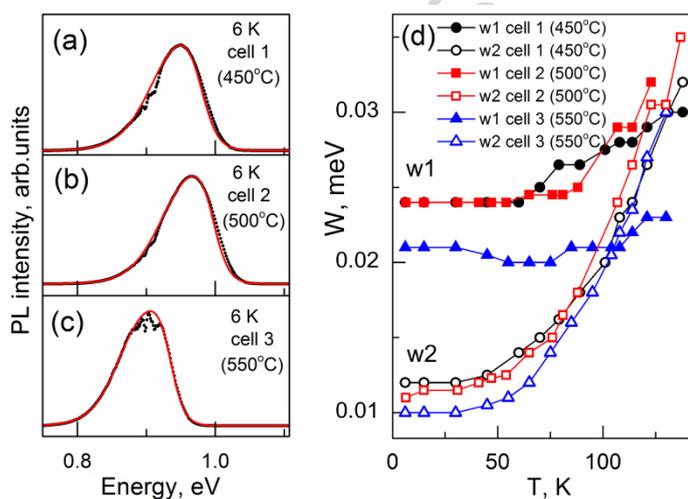
Fig. 5. The PL spectra (shown by symbols) of solar cell 1 (a), 2 (b) and 3 (c), taken at 6 K, fitted with asymmetric double sigmoidal functions (shown by red solid lines), Temperature dependence of fitting parameters W1 and W2 (d).

The P3 band appears in our PL spectra after the deposition of CdS and ZnO suggesting that it could be related either to CdS or to ZnO. Bands at 1.3 eV, observed in PL spectra of Zn excess CZTSe films on glass [3] and on Mo/glass [14,17] substrates, have been reported earlier and assigned to defects in ZnSe [17] assuming sub-bandgap

excitation due to high concentration of defects. Such emission might also be present in our PL spectra as a high energy tail. However, its intensity in the PL spectra of the as deposited CZTSe films is significantly lower than that of the P3 band appearing after processing as it can be seen in Fig.8.
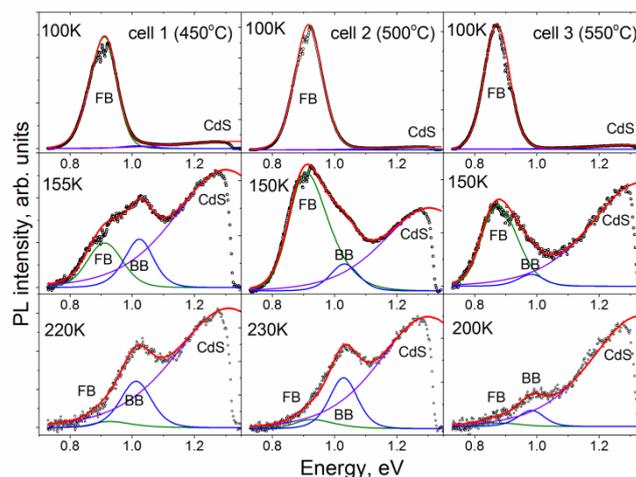
Fig. 6. PL spectra, measured at different temperatures, fitted with DSF. Column 1 - solar cell 1, column 2 - solar cell 2, column 3 - solar cell 3.

Arrhenius analysis of the temperature quenching of the dominant bands in the PL spectra was carried out using their integrated intensities. Arrhenius plots of the resulting intensities for the three solar cells are shown in Fig. 7. The best fits have been achieved for a single recombination channel and assuming a temperature dependence of the hole capture cross section proposed in [18] $I(T) = I_0/[1+A_1T^{3/2}+A_2T^{3/2}exp(-E_a/k_BT)]$, where I_0 is the P1 band integrated intensity at the lowest temperature of 6 K, and A_1 and A_2 are process rate parameters.

Arrhenius analysis of the temperature quenching shows a gradual increase of the activation energy from 65±5 meV for cell 1 (450°C) to 70±5 meV for cell 2 (500°C) and 75±5 meV for cell 3 (550°C). These activation energies are also shown in Table 2.

All the three activation energies are greater than γ suggesting that the P1 dominant band in all the three solar cells is the free-to-bound (FB) transition involving the recombination of free electrons with holes localised at acceptors.

Fig.8 shows a comparison of the PL spectra, measured at 6 K in similar optical conditions for as deposited CZTSe films on Mo/glass substrates, reported in ref. [2], with the spectra measured for solar cells 1, 2 and 3 in this study. It can be seen that the solar cell processing for all the three cells results in an increase of the PL intensity and a blue shift of the band. The most prominent effect can be seen for film 2 selenised at 500°C. The PL intensity has increased by about 73% along with a blue shift of 15 meV. A smaller increase in the emission intensity by 22% and a blue shift of P1 by 10 mV can be seen for film 1.
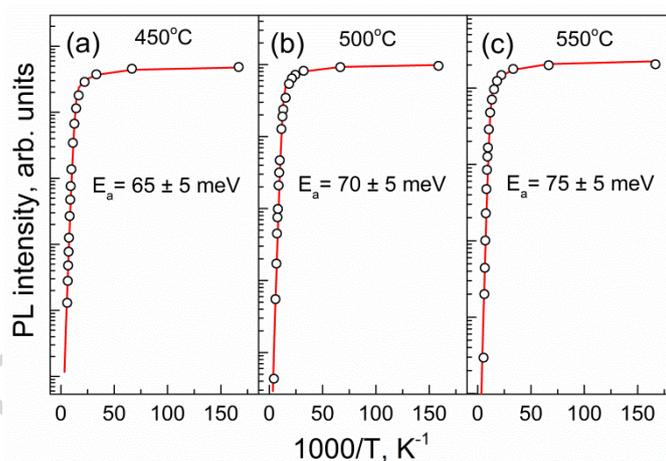
Fig. 7. Arrhenius plots of the integrated intensities of the FB bands in the PL spectra of solar cells 1(a), 2 (b) and 3(c).

The small increase of the emission intensity of 10% observed for the PL spectra of film 3 might also be a result of the processing. Parameters of the PL spectra for the films and cells are shown in Table 2. The observed changes in the PL spectra are an integrated effect of the processing: KCN etching, deposition of CdS, resulting in the

formation of *p-n* junction and low temperature (70°C) heating as well as deposition of ZnO layers which also might include effects of non-intentional heating of the films. In the frame of this optical study it is rather difficult to establish the nature of each particular effect however below we will try to speculate on the origin of the observed changes in the optical properties.

The increase of the emission intensity can be assigned to a reduction of the concentration of non-radiative recombination centers on the surface due to the etching. However such an increase and the blue shifts of the dominant band can partly be attributed to changes in doping conditions in the near surface layer due to inter-diffusion of Cd, S, Se and Zn taking place after the deposition of CdS [19]. The chemistry of such an inter-diffusion should critically depend on the elemental composition, defining the defect content in the near surface layer. This results in the observed differences in E_g increasing from 1.05 eV to 1.06 eV after the processing of film 1 whereas E_g of film 2 and 3 becomes smaller after the processing (falling from 1.03 eV to 1.02 eV and from 1.05 eV to 1.02 eV, respectively).

The processing did not change the k parameters, which suggests that the recombination mechanism of the dominant band is still FB. However the *j*-shift of the cells, reflecting the compensation level of CZTSe, becomes greater after the processing, and could be due to the formation of new donors in the interface layer. This is consistent with the formation of an interface layer with inter-diffused elements Cd, S, Se and Zn. A theoretical analysis of the cadmium on copper site Cd_{Cu} antisite defects in CZTSe demonstrate that such defects have small formation energy and are likely to be donors [20]. The processing of film 1 and film 2 does not change their mean depth of potential

fluctuations of 24 meV whereas such a processing reduces γ in film 3 from 27 meV to 21 meV. This may mean that the defects, associated with the band-tails, are not related to the non-radiative traps reducing the intensity of PL emission.
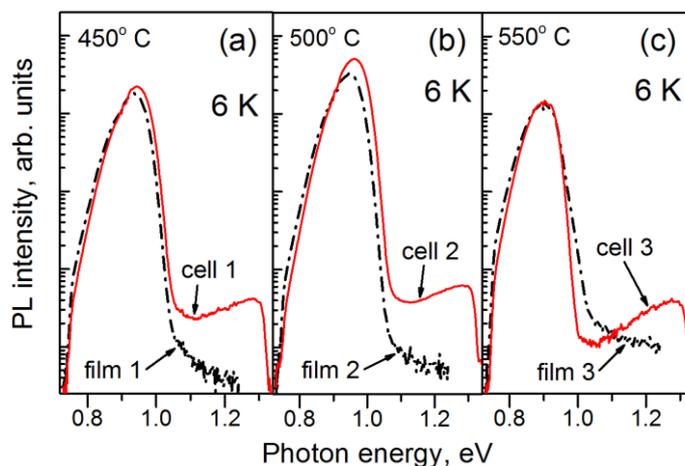
Fig. 8. A comparison of the PL spectra measured at 6 K in as deposited CZTSe films 1, 2 and 3, selenised at 450°C (a), 500°C (b), 550°C (c), respectively, and solar cells 1, 2 and 3 fabricated from these films.

The activation energies of the temperature quenching of the P1 band in the PL spectra of the as deposited CZTSe films reported in ref. [3] were determined after the decomposition of the PL spectra by fitting Gaussians. In this study we used more accurate DSF functions. Such an accurate fitting resulted in slightly different E_a shown in Table 2. Therefore we compare E_a, determined for the films after the processing, with the new more accurate values. The processing increases E_a for all the three films which might be associated with an increase in the energy depth of the dominant acceptor after the solar cell fabrication process.

The presence of a *p-n* junction in the ZnO/CdS/CZTSe/Mo cells results in the formation of a space charge layer (SCL) whose thickness we roughly estimate as 0.3 μm

[21]. Assuming an absorption coefficient of $5x10^4$ cm^{-1} for CZTSe [22] we also can estimate the thickness of the layer, excited by the laser, to be of 0.2 µm. So the PL in our cells can be influenced by SCL. However at the open circuit condition charge carriers, photo-injected by the laser excitation, drastically reduce the electric fields in SCL reducing its magnitude and thickness [23]. Therefore the influence of the *p-n* junction on the PL spectra might not be significant. This is supported by the similarity of the *k*-parameter of the dominant band P1 before and after the processing.

4. Conclusion

The effect of solar cell processing, including etching in KCN along with deposition of CdS and ZnO, of CZTSe films, fabricated by selenising metallic precursors at 450°C (film 1), 500°C (film 2) and 550°C (film 3), was studied using photoluminescence (PL) and photoluminescence excitation (PLE). Analysis of the temperature and excitation intensity dependence of the P1 dominant PL band in the PL spectra of the solar cells suggests the free-to-bound (FB) recombination of free electrons with holes localised at deep acceptor levels influenced by valence band-tails. This mechanism is similar to that for the dominant band in the PL spectra of the as deposited CZTSe films. Solar cell processing increased the intensity of P1 and blue shifted it. The strongest increase in the intensity and blue shift was observed for film 2, selenised at 500°C. A smaller intensity increase and blue shift was found for film 1, selenised at 450°C, whereas only a slight intensity rise was found for film 3. The intensity increase we assign to a reduction of the concentration of non-radiative recombination centers on the surface after the etching and inter-diffusion of Cd, S, Se and Zn, taking place after the deposition of CdS.

Processing increased E_g, measured at 4.2 K, in film 1, whereas in film 2 and 3 E_g became smaller. The rate of the P1 shift (j-shift) with excitation power rise increased for all films suggesting a rise of the compensation degree. These are consistent with the formation of an interface layer with the inter-diffused elements forming new donors (Cd_{Cu}). The chemistry of inter-diffusion depends on the elemental composition, defining the defect content and influencing E_g. The average depth of potential fluctuations γ of 24 meV in film 1 and 2 remained unchanged after processing, whereas in film 3 γ decreased from 27 meV to 21 meV.

Acknowledgements

References

[1] X. Liu, Y. Feng, H. Cui, F. Liu, X. Hao, G. Conibeer, D.B. Mitzi, M. Green, The current status and future prospects of kesterite solar cells: a brief review, Prog. Photovolt. 24 (2016) 879.

[2] Y.S. Lee, T. Gershon, O. Gunawan, T.K. Todorov, T. Gokmen, Y. Virgus, S. Guha, $Cu_2ZnSnSe_4$ Thin-Film Solar Cells by Thermal Co-evaporation with 11.6% Efficiency and Improved Minority Carrier Diffusion Length, Advanced Energy Materials, 12 (2015) 1401372.

[3] J. Márquez-Prieto, M.V. Yakushev, I. Forbes, J. Krustok, V.D. Zhivulko, P.R. Edwards, M. Dimitrievska, V. Izquerdo-Roca, N.M. Pearsall, A.V. Mudryi, R.W. Martin, Impact of the selenisation temperature on the structure and optical properties of CZTSe absorbers, Sol. Energy Mater. Sol. Cells 152 (2016) 42.

[4] H.B. Bebb, E. Williams, Semiconductors and Semimetals, Academic Press, New York, 8 (1972) p. 181.

[5] M. Grossberg, J. Krustok, K. Timmo, M. Altosaar, Radiative recombination in $Cu_2ZnSnSe_4$ monograins studied by photoluminescence spectroscopy, Thin Solid Films, 517 (2009) 2489-2492.

[6] T. Gokmen, O. Gunawan, T. K. Todorov, D. B. Mitzi, Band tailing and efficiency limitation in kesterite solar cells, Appl.Phys. Lett.103 (2013) 103506.

[7] C. Persson, Electronic and optical properties of Cu_2ZnSnS_4 and $Cu_2ZnSnSe_4$, Journal of Applied Physics, 107 (2010) 053710.

[8] J.P. Teixeira, R.A. Sousa, M.G. Sousa, A.F. da Cunha, P.A. Fernandes, P.M.P. Salomé, J.P. Leitão, Radiative transitions in highly doped and compensated chalcopyrites and kesterites: The case of Cu_2ZnSnS_4, Phys. Rev. B 90 (2014) 235202.

[9] A.P. Levanyuk, V.V. Osipov, Edge luminescence of direct-gap semiconductors, Sov. Phys. Usp. 24 (1981) 187.

[10] J. Krustok, H. Collan, M. Yakushev, K. Hjelt, The Role of Spatial Potential Fluctuations in the Shape of the PL Bands of Multinary Semiconductor Compounds, Phys. Scr. T79 (1999) 179.

[11] M.V. Yakushev, M.A. Sulimov, J. Márquez-Prieto, I. Forbes, J. Krustok, P.R. Edwards, V.D. Zhivulko, O.M. Borodavchenko, A.V. Mudryi, R.W. Martin, Influence

of the copper content on the optical properties of CZTSe thin films, Sol. Energy Mater. Sol. Cells 168 (2017) 69.

[12] J. Márquez-Prieto, Y. Ren, R.W. Miles, N. Pearsall, I. Forbes, The influence of precursor Cu content and two-stage processing conditions on the micro-structure of $Cu_2ZnSnSe_4$, Thin Solid Films 582 (2015) 220.

[13] T. Schmidt, K. Lischka, W. Zulehner, Excitation-power dependence of the near-band edge photoluminescence of semiconductors, Phys. Rev. B 45 (1992) 8989.

[14] M.V. Yakushev, J. Márquez-Prieto, I. Forbes, P.R. Edwards, V.D. Zhivulko, A.V. Mudryi, J. Krustok, R.W. Martin, Radiative recombination in $Cu_2ZnSnSe_4$ thin films with Cu deficiency and Zn excess, Journal of Physics D: Applied Physics, 48 (2015) 475109.

[15] K.P. O'Donnell, R.W. Martin, P.G. Middleton, Origin of luminescence from InGaN Diodes, Phys. Rev. Lett. 82 (1999) 237.

[16] M.E. White, K.P. O' Donnell, R.W. Martin, S. Pereira, C.J. Deatcher, I.M. Watson, Photoluminescence excitation spectroscopy of InGaN epilayers, Mater. Sci. Eng. B 93 (2002) 147.

[17] R. Djemour, M. Mousel, A. Redinger, L. Gütay, A. Crossay, D. Colombara, P. J. Dale, S. Siebentritt, Detecting ZnSe secondary phase in Cu2ZnSnSe4 by room temperature photoluminescence, Appl. Phys. Lett. 102 (22) 222108.

[18] J. Krustok, H. Collan, K. Hjelt, Does the low-temperature Arrhenius plot of the photoluminescence intensity in CdTe point towards an erroneous activation energy? J. Appl. Phys. 3 (1997) 1442.

[19] M. Bar, I. Repins, L. Weinhardt, J.-H. Alsmeier, S. Pookpanratana, M. Blum, W. Yang, C. Heske, R.G. Wilks, and R. Noufi, Zn−Se−Cd−S Interlayer Formation at the CdS/$Cu_2ZnSnSe_4$ Thin-Film Solar Cell Interface, ACS Energy Lett. 2 (2017) 1632.

[20] T. Maeda, S. Nakamura, T. Wada, First-Principles Study on Cd Doping in Cu_2ZnSnS_4 and $Cu_2ZnSnSe_4$, Jap. J. Appl. Phys. 51 (2012) 10NC11.

[21] S. Ranjbar, G. Brammertz, B. Vermang, A. Hadipour, M. Sylvester, A. Mule, M. Meuris, A.F. da Cunha, J. Poortmans, Effect of Sn/Zn/Cu precursor stack thickness on two-step processed kesterite solar cells, Thin Solid Films, 633 (2017) 127.

[22] M.I. Amal, K.H. Kim, Optical properties of selenised $Cu_2ZnSnSe_4$ films from a Cu-Zn-Sn metallic precursor, Chalcogenide Lett. **9** (2012) 345.

[23] W. K. Metzger, R. K. Ahrenkiel, J. Dashdorj, and D.J. Friedman, Analysis of charge separation dynamics in a semiconductor junction, Phys. Rev. B 71 (2005) 035301.

Highlights

- Cu$_2$ZnSnSe$_4$ (CZTSe) films on Mo/glass were produced by selenisation of metallic precursors

- PL temperature and excitation intensity dependencies are analysed.

- The bandgaps are determined using PLE.

- PL bands are identified as free-to-bound and band-to-band transitions.